

Vortex states of the E_u model for Sr_2RuO_4

Takafumi Kita

Division of Physics, Hokkaido University, Sapporo 060-0810, Japan

(February 5, 2020)

Based on the Ginzburg-Landau functional of E_u symmetry presented by Agterberg, vortex states of Sr_2RuO_4 are studied in detail over $H_{c1} \lesssim H \leq H_{c2}$ by using the Landau-level expansion method. For the field in the basal plane, it is found that (i) the second superconducting transition should be present irrespective of the field direction; (ii) below this transition, a characteristic double-peak structure may develop in the magnetic-field distribution; (iii) a third transition may occur between two different vortex states. It is also found that, when the field is along the c axis, the square vortex lattice may deform through a second-order transition into a rectangular one as the field is lowered from H_{c2} . These predictions will be helpful in establishing the E_u model for Sr_2RuO_4 .

After Rice and Sigrist [1] pointed out the possibility of p -wave pairing, much attention has been focused on the superconducting Sr_2RuO_4 which was discovered by Maeno *et al.* [2]. This material has the same layered perovskite structure as La_2CuO_4 with a rather low transition temperature $T_c \approx 1.5\text{K}$, and the irreducible representation E_u has been raised and discussed in detail as a possible candidate for the pairing symmetry [3]. There are experimental indications for the identification: strong dependence of T_c on non-magnetic impurities [4]; absence of the Hebel-Slichter peak in NQR-experiments [5]; no temperature dependence of the Knight shift through T_c for $\mathbf{H} \perp \hat{\mathbf{c}}$ [6]; anomalous temperature dependence of the tunneling current [7] whose features have been reproduced by the E_u model [8,9]; increase of the relaxation rate below T_c in a zero-field μSR experiment [10]. However, further experiments seem being required before establishing the validity of the E_u model for Sr_2RuO_4 . Especially, the vortex states may provide clear and indisputable tests for the p -wave hypothesis. The present paper provides a detailed theoretical description of the vortex states which will be helpful towards that purpose.

The vortex states of the E_u model for Sr_2RuO_4 have been studied theoretically in a series of papers by Agterberg *et al.* [11–13]. Based on the two-component Ginzburg-Landau (GL) functional and following essentially Abrikosov's method [14] which is effective near the upper (H_{c2}) and lower (H_{c1}) critical fields, they have provided several important predictions. Especially noteworthy among them are: existence of the second transition for $\mathbf{H} \perp \hat{\mathbf{c}}$ similar to that observed in UPt_3 [15,16]; several orbital-dependent phenomena helpful in identifying which band is mainly relevant; stabilization of the square vortex lattice for $\mathbf{H} \parallel \hat{\mathbf{c}}$. The observation of a square vortex lattice has been reported by Riseman *et al.* [17].

With these results, the aims of the present paper are the following: (i) The properties of the intermediate fields, in particular those below the second transition for $\mathbf{H} \perp \hat{\mathbf{c}}$, remain to be clarified. We will treat the whole range $H_{c1} \leq H \leq H_{c2}$ in a unified way, describe possible changes of experimentally detectable properties as a function of the field strength, and draw characteristic

properties in low fields. (ii) Considered have been the cases where the field is applied along the high-symmetry axes. It is still not clear whether or not the second transition for $\mathbf{H} \perp \hat{\mathbf{c}}$ persists for arbitrary field directions in the ab plane, because the term $|\eta_1|^2|\eta_2|^2$ in the GL functional [see Eq. (1) below] generally causes the first- and third-order mixing. We will study those general cases to show the existence of the second transition for an arbitrary direction in the ab plane. (iii) Agterberg introduced several assumptions in the parameters used to minimize the free energy. We will perform the minimization without such assumptions. It should be noted that the results obtained here for $\mathbf{H} \perp \hat{\mathbf{c}}$ are qualitatively applicable to UPt_3 so that they will also be useful for the experiments of UPt_3 .

The goals (i)-(iii) may seem rather formidable, but they can be achieved with the Landau-level expansion method [18]. When applied to the s -wave pairing, it successfully reproduced the properties of the whole region $H_{c1} \lesssim H \leq H_{c2}$ quite efficiently for an arbitrary κ . Compared with the direct minimization procedure in real space [19], the method has a couple of advantages that (i) it is far more efficient and (ii) one can enumerate possible second-order transitions rather easily, hence enabling us to establish the phase diagram for various multi-order-parameter systems. The method can also be used in solving the Bogoliubov-de Gennes equations to study the vortex states microscopically [20]. This is the first time where it is applied to multi-order-parameter systems so that the present paper also has some methodological importance.

The GL free-energy density adopted by Agterberg is given by [11]

$$f = -|\boldsymbol{\eta}|^2 + \frac{1}{2}|\boldsymbol{\eta}|^4 + \frac{\gamma}{2}|\boldsymbol{\eta} \times \boldsymbol{\eta}^*|^2 + (3\gamma - 1)|\eta_1|^2|\eta_2|^2 + \boldsymbol{\eta}^\dagger \begin{bmatrix} D_x^2 + \gamma D_y^2 + \kappa_5 D_z^2 & \gamma(D_x D_y + D_y D_x) \\ \gamma(D_x D_y + D_y D_x) & D_y^2 + \gamma D_x^2 + \kappa_5 D_z^2 \end{bmatrix} \boldsymbol{\eta} + h^2, \quad (1)$$

where the same notations as ref. [11] are used here. This

simplified free energy, which can be obtained from the weak-coupling theory, has the advantage that there are only two parameters in it whose values can be extracted from experiments, i.e. $\kappa_1 \equiv H_{c2}/\sqrt{2}H_c$ and $\nu \equiv \frac{1-\gamma}{1+\gamma}$ which is related to the anisotropy of H_{c2} in the ab plane through $H_{c2}(\mathbf{a})/H_{c2}(\mathbf{a} + \mathbf{b}) = (1 - \nu)/(1 + \nu)$ [11]. The value $\kappa_1 = 31$ (1.2) for $\mathbf{H} \perp \hat{\mathbf{c}}$ ($\mathbf{H} \parallel \hat{\mathbf{c}}$) will be used throughout [21], whereas ν is left as a parameter. A recent observation of the H_{c2} anisotropy in the ab plane suggests ν is positive and ~ 0.01 [22].

We sketch the method to find the minimum for an arbitrary field strength [18]. Let us fix the mean flux density $\mathbf{B} \equiv (B \sin \theta \cos \varphi, B \sin \theta \sin \varphi, B \cos \theta)$ rather than the external field H , and express $\mathbf{h} = \mathbf{B} + \tilde{\mathbf{h}}$ where the spatial average of $\tilde{\mathbf{h}}$ vanishes by definition. We then perform the transformations:

$$\begin{bmatrix} x \\ y \\ z \end{bmatrix} = \begin{bmatrix} \cos \theta \cos \varphi & -\sin \varphi & \sin \theta \cos \varphi \\ \cos \theta \sin \varphi & \cos \varphi & \sin \theta \sin \varphi \\ -\sin \theta & 0 & \cos \theta \end{bmatrix} \begin{bmatrix} x'/L \\ y'L \\ z' \end{bmatrix}, \quad (2)$$

$$\boldsymbol{\eta}(\mathbf{r}) = \begin{bmatrix} \cos \frac{\phi}{2} & -\sin \frac{\phi}{2} \\ \sin \frac{\phi}{2} & \cos \frac{\phi}{2} \end{bmatrix} \boldsymbol{\eta}'(\mathbf{r}'), \quad (3)$$

where the rotation angle ϕ and the scaling factor L are conveniently chosen as $\phi = \tan^{-1} \left(\frac{2\gamma}{1-\gamma} \tan 2\varphi \right)$ and $L = \left[\frac{1+\gamma-f}{(1+\gamma-f) \cos^2 \theta + \kappa_5 \sin^2 \theta} \right]^{1/4}$ with $f \equiv [(1-\gamma)^2 \cos^2 2\varphi + 4\gamma^2 \sin^2 2\varphi]^{1/2}$. Assuming uniformity along the $\hat{\mathbf{z}}'$ direction, we now expand $\boldsymbol{\eta}'(\mathbf{r}')$ and $\tilde{\mathbf{h}}(\mathbf{r}')$ as

$$\boldsymbol{\eta}'(\mathbf{r}') = \sqrt{V} \sum_{N\mathbf{q}} \mathbf{c}_{N\mathbf{q}} \psi_{N\mathbf{q}}(\mathbf{r}'), \quad (4)$$

$$\tilde{\mathbf{h}}(\mathbf{r}') = \hat{\mathbf{z}}' \sum_{\mathbf{K} \neq 0} \tilde{h}_{\mathbf{K}} \exp(i\mathbf{K} \cdot \mathbf{r}'), \quad (5)$$

where V is the volume of the system, $\psi_{N\mathbf{q}}$ denotes an eigenstate of the magnetic translation group in the flux density B carrying the Landau-level index N and the magnetic Bloch vector \mathbf{q} , and \mathbf{K} is the reciprocal lattice vector of the vortex lattice. The explicit expression of $\psi_{N\mathbf{q}}(\mathbf{r}')$ for the spacial case where one of the unit vectors of the vortex lattice, \mathbf{a}_2 , lies along the y' axis is given by

$$\begin{aligned} \psi_{N\mathbf{q}}(\mathbf{r}') &= \sum_{n=-N_f/2+1}^{N_f/2} e^{i[q_{y'}(y'+0.5q_{x'}) + na_{1x'}(y'+q_{x'}-0.5na_{1y'})]/l_c^2} \\ &\times \sqrt{\frac{2\pi l_c/a_2}{2^N N! \sqrt{\pi} V}} H_N \left(\frac{x' - q_{y'} - na_{1x'}}{l_c} \right), \end{aligned} \quad (6)$$

with N_f^2 the number of vortices in the system, l_c denoting $\frac{1}{\sqrt{2}}$ of the magnetic length, and $a_{1x'}$ ($a_{1y'}$) the x' (y') component of another unit vector \mathbf{a}_1 [18]. In the actual

calculations we have also considered the counterclockwise rotation of \mathbf{a}_1 and \mathbf{a}_2 around the z' axis by the angle φ'_L . Substituting Eqs. (2)-(6) into Eq. (1) and integrating over the volume, we obtain the free energy per unit volume as

$$F[\{\mathbf{c}_{N\mathbf{q}}\}, \{\tilde{h}_{\mathbf{K}}\}, B, \rho, \vartheta, \varphi'_L] = \frac{1}{V} \int f[\boldsymbol{\eta}'(\mathbf{r}'), \tilde{\mathbf{h}}(\mathbf{r}'), B] d^3 r' \quad (7)$$

where $\rho \equiv |\mathbf{a}_1|/|\mathbf{a}_2|$ and $\vartheta \equiv \cos^{-1} \frac{\mathbf{a}_1 \cdot \mathbf{a}_2}{|\mathbf{a}_1||\mathbf{a}_2|}$. This F is the desired functional which can be minimized rather easily using one of the standard minimization algorithms [23]. Due to the periodicity of the vortex lattice, we only have to perform the integration over a unit cell. The external field H is then determined through the thermodynamic relation ($H = \frac{1}{2} \frac{\partial F}{\partial B}$ in the present units). In numerical calculations we have cut the series in Eqs. (4) and (5) at some N_c and $|\mathbf{K}_c|$, respectively, thereby obtaining a variational estimate of the free energy. The convergence can be checked by increasing N_c and $|\mathbf{K}_c|$. The choice $N_c \sim 12$ and $\mathbf{K}_c \sim$ (the third smallest) has been checked to provide correct identification of the free-energy minimum with the relative accuracy of 10^{-6} for $B/H_{c2} \gtrsim 0.1$. Though not presented here, preliminary calculations reveal that the method is also effective for $\theta \neq 0$.

The functional F has another advantage that one may enumerate possible transitions in the vortex states of multi-order-parameter systems. Much attention has been focused on this subject in connection with the observed phase diagram of superconducting UPt_3 [24]. No complete analysis has appeared yet, however, and the use of F will be quite helpful for that purpose. (In this connection it is worth pointing out the same idea of using the expansion coefficients rather than the order parameter itself was already adopted by Landau in his classic paper of the second-order transition [25].) Now, the features of the s -wave vortex lattice can be summarized as follows [18]: (a) a single \mathbf{q} in Eq. (4) suffices to describe it with a choice of \mathbf{q} corresponding to the broken translational symmetry of the lattice; (b) the hexagonal (square) lattice is made up of $N = 6n$ ($4n$) Landau levels (n : integer) [26,18]; (c) more general structures can be described by $N = 2n$ levels, with odd N 's never mixing up since those bases have finite amplitude at the core sites; (d) the expansion coefficients $\mathbf{c}_{N\mathbf{q}}$ can be chosen as real for the hexagonal and square lattices. With these results on the conventional lattice, the following second-order transitions are possible in multi-component systems: (i) the deformation of the hexagonal or square lattice which accompanies entry of new N 's as well as imaginary numbers in the expansion coefficients; (ii) mixing of another wave number \mathbf{q}_2 satisfying $\mathbf{q}_2 - \mathbf{q}_1 = \mathbf{K}/2$ as considered by Garg and Chen [27], which makes the vortex state coreless; (iii) entry of odd N 's. Though not complete, this consideration will be sufficient below.

We now present the results for $\mathbf{H} \perp \hat{\mathbf{c}}$. Figure 1 shows the transition lines for $\mathbf{H} \parallel \hat{\mathbf{a}}$ ($\theta = \frac{\pi}{2}$; $\varphi = 0$) as a function of the anisotropy parameter ν ; the one given as a func-

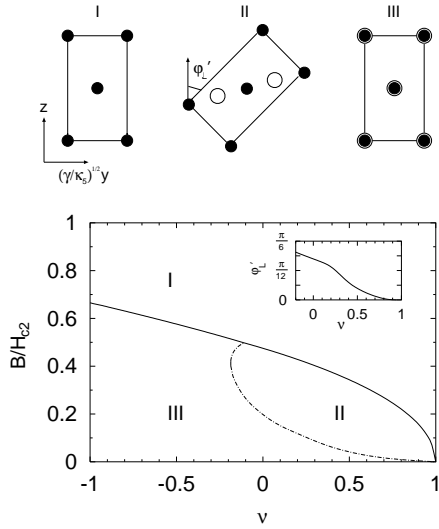


FIG. 1. Transition lines for $\mathbf{H} \perp \hat{\mathbf{a}}$ as a function of the anisotropy parameter ν . The closed (open) circles denote the zeros of η_1 (η_2). The inset plots the angle φ'_L at the I \leftrightarrow II transition as a function of ν .

tion of $\gamma = \frac{1-\nu}{3+\nu}$ has qualitatively the same structure, with $\gamma=0$ and 1 respectively corresponding to $\nu=1$ and -1 . As already pointed out by Agterberg [11], there are three possible vortex states: the high-field region I where a hexagonal lattice is stable with $\eta_2 = 0$; the region II where η_2 becomes finite with $\mathbf{q}_2 - \mathbf{q}_1$ equal to half the unit vector \mathbf{b}_1 of the reciprocal lattice, i.e. the vortex lattice is coreless with $|\boldsymbol{\eta}|$ finite everywhere; the region III where a deformed conventional lattice with $\eta_2 \neq 0$ is stable. Figure 1, however, includes the following new results: (i) a full minimization with respect to φ'_L clarifies that the I \leftrightarrow II transition is continuous as a function of ν or γ (see the inset); (ii) high-precision calculations in the low-field region reveal that, as the field is lowered, the coreless state II is replaced via a first-order transition by the state III with cores. The present method also enables us to perform a detailed study on the properties below the second transition. The reason for (ii) can thereby be realized by looking at the variation of $l_z \equiv (\boldsymbol{\eta} \times \boldsymbol{\eta}^*) \cdot \hat{\mathbf{z}} / 2i|\eta_1||\eta_2|$ in the state II which is proportional to the magnitude of the orbital angular momentum along $\hat{\mathbf{z}}$. As seen in Fig. 2 calculated for $\nu=0.077$ ($\gamma=0.3$) and $B/H_{c2}=0.25$, there are lines of “defects” in the state II where l_z vanishes. Compared with III where $|\boldsymbol{\eta}|$ vanishes at points, the state II is thus energetically unfavorable at low fields. It can however be stabilized at intermediate fields by making $|\boldsymbol{\eta}|$ more uniform. Figure 3 plots $|\boldsymbol{\eta}(\mathbf{r})|$ for $\nu = 0.077$, clarifying how the differences between II and III develop as B/H_{c2} is decreased: only a deformation of the lattice occurs in the state III, whereas a layered structure also develops in the state II with $|\boldsymbol{\eta}(\mathbf{r})|$ becoming more and more uniformly distributed. This rather drastic change in II can be detected by measuring the magnetic-field distribution $P(h) \equiv \frac{1}{V} \int \delta[h - h_x(\mathbf{r})] d^3r$. As seen in Fig. 4, the single peak for $B/H_{c2}=0.45$ splits and one of them

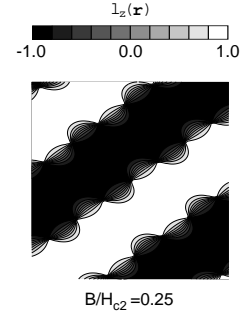


FIG. 2. Spatial variation of $l_z \equiv (\boldsymbol{\eta} \times \boldsymbol{\eta}^*) \cdot \hat{\mathbf{z}} / 2i|\eta_1||\eta_2|$ in the state II for $\nu = 0.077$ and $B/H_{c2} = 0.25$. The region with $l_z \approx \pm 1$ corresponds to the “bulk” state. See Fig. 3 for the corresponding $|\boldsymbol{\eta}(\mathbf{r})|$.

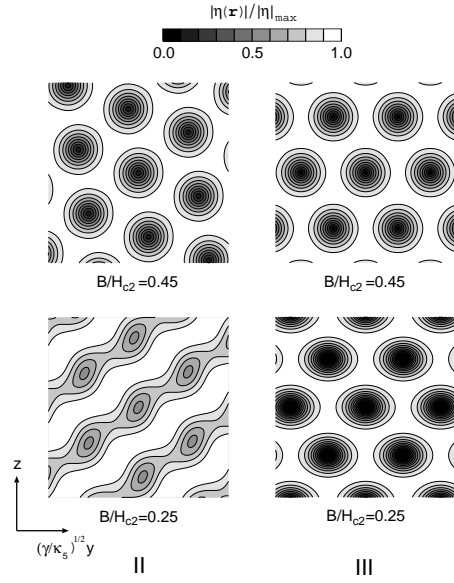


FIG. 3. A comparison of $|\boldsymbol{\eta}(\mathbf{r})|$ between the states II and III with $\nu = 0.077$ and $B/H_{c2} = 0.45, 0.25$. $|\boldsymbol{\eta}(\mathbf{r})|$ is finite everywhere in the state II, which is brought about at the expense of the variation in l_z ; see Fig. 2.

moves towards the high-field end. This change can be attributed to the development of a ridge in $h_x(\mathbf{r})$ along a valley of $|\boldsymbol{\eta}(\mathbf{r})|$. The observation of it by NMR or μ SR experiments will form a direct evidence for the state II as well as for the presence of multi-order parameters. It is also quite interesting to perform the experiments in UPt_3 where a lattice distortion has already been detected [28]. The possibility of observing the splitting may be much higher here, which will provide quite an important clue to clarify its H - T phase diagram since the transition of $\mathbf{q}_2 - \mathbf{q}_1 \neq 0$ persists irrespective of the field directions. Going back to Sr_2RuO_4 , we finally point out that the second-order transition between I \leftrightarrow II or I \leftrightarrow III is present for an arbitrary field direction in the basal plane. A glance on the functional (1) may lead to the conclusion that the transition I \leftrightarrow III disappears for a low-symmetry

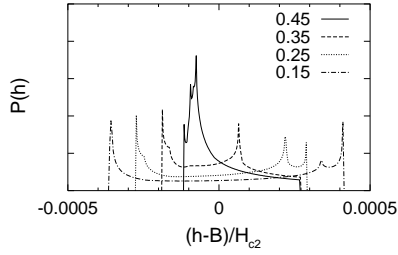


FIG. 4. The magnetic-field distribution $P(h)$ in the state II for $B/H_{c2} = 0.45, 0.35, 0.25$, and 0.15 . A characteristic double-peak structure develops as the field is decreased.

direction, since the term $|\eta_1|^2|\eta_2|^2$ yields those like $\eta_1'\eta_2'^*|\eta_1'|^2$. However, it does persist as the transition (i) in the classification of the preceding paragraph. The hexagonal lattice has been checked to be stable in the high-field region, and the phase diagram for a small $|\nu|$ is qualitatively similar to Fig. 1.

We finally present the results for $\mathbf{H} \parallel \hat{\mathbf{c}}$. Figure 5 shows the vortex lattice structure as a function of the anisotropy parameter ν and the flux density B for $\kappa_1 = 1.2$. A square lattice is stabilized near H_{c2} for small values of $|\nu|$, confirming Agterberg's result through a perturbation expansion with respect to ν ($\kappa_1 = 1.2$ corresponds Agterberg's $\kappa \sim 0.54$ for $\nu = 0$) [12]. As the field is decreased, however, the lattice deforms through a second-order transition into a rectangular one for $|\nu| \lesssim 0.1$. The inset plots how the distortion develops for the special case of $\nu = 0$, showing a feature characteristic of the second-order transition. The same calculation carried out for $\kappa_1 = 1.8$ clarifies that the transition line, though shifting downward, still persists. For small values of κ_1 and $|\nu|$, the free energies of the square, rectangular, and hexagonal lattices are not much different from one another, as suggested by Agterberg's ν - κ diagram near H_{c2} [12], and the present calculation

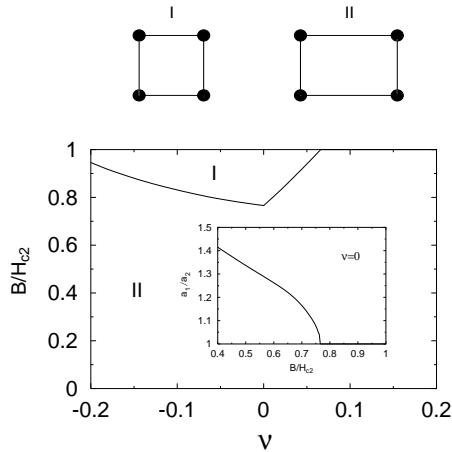


FIG. 5. Transition lines for $\mathbf{H} \perp \hat{\mathbf{c}}$ as a function of ν . The square (rectangular) lattice is stable in the region I (II). The closed circles denote the zeros of $|\eta|$. The inset plots $|a_1|/|a_2|$ as a function of B/H_{c2} for the case $\nu = 0$.

reveals that there may also be a field-dependent transformation among them. Although Riseman *et al.* [17] have reported an observation of the square lattice, there may exist a little distortion in the diffraction pattern which is field dependent. A detailed experiment on the field dependence may be worth carrying out.

The author is grateful to M. Sigrist for several useful conversations. Numerical calculations were performed on an Origin 2000 in "Hierarchical matter analyzing system" at the Division of Physics, Graduate School of Science, Hokkaido University.

-
- [1] T. M. Rice and M. Sigrist, J. Phys. **7**, L643 (1995).
 - [2] Y. Maeno *et al.*, Nature **372**, 532 (1994).
 - [3] D. F. Agterberg, T. M. Rice, and M. Sigrist, Phys. Rev. Lett. **78**, 3374 (1997).
 - [4] A. P. Mackenzie *et al.*, Phys. Rev. Lett. **80**, 161 (1998).
 - [5] K. Ishida *et al.*, Phys. Rev. B **56**, R505 (1997).
 - [6] K. Ishida *et al.*, Nature **396**, 658 (1998).
 - [7] R. Jin *et al.*, Phys. Rev. B **59**, 4433 (1999).
 - [8] C. Honerkamp and M. Sigrist, Prog. Theor. Phys. **100**, 53 (1998).
 - [9] M. Yamashiro, Y. Tanaka, and S. Kashiwaya, J. Phys. Soc. Jpn. **67**, 3364 (1998).
 - [10] G. M. Luke *et al.*, Nature **394**, 558 (1998).
 - [11] D. F. Agterberg, Phys. Rev. Lett. **80**, 5184 (1998).
 - [12] D. F. Agterberg, Phys. Rev. B **58**, 14484 (1998).
 - [13] R. Heeb and D. F. Agterberg, Phys. Rev. B **59**, 7076 (1999).
 - [14] A. A. Abrikosov, Zh. Eksp. Teor. Fiz. **32**, 1442 (1957) [Sov. Phys. JETP **5**, 1174 (1957)].
 - [15] G. Bruls *et al.*, Phys. Rev. Lett. **65**, 2294 (1990).
 - [16] S. Adenwalla *et al.*, Phys. Rev. Lett. **65**, 2298 (1990).
 - [17] T. M. Riseman *et al.*, Nature **396**, 242 (1998).
 - [18] T. Kita, J. Phys. Soc. Jpn. **67**, 2067 (1998).
 - [19] K. Machida, T. Fujita, and T. Ohmi, J. Phys. Soc. Jpn. **62**, 680 (1993).
 - [20] T. Kita, J. Phys. Soc. Jpn. **67**, 2075 (1998).
 - [21] K. Yoshida *et al.*, J. Phys. Soc. Jpn. **65**, 2220 (1996).
 - [22] Z. Q. Mao, T. Akima, T. Ando, and Y. Maeno, unpublished.
 - [23] See, e.g. W. H. Press, S. A. Teukolsky, W. T. Vetterling and B. P. Flannery: *Numerical Recipes in C* (Cambridge University Press, Cambridge, 1988) Chap. 10.
 - [24] See, e.g. M. Sigrist and K. Ueda, Rev. Mod. Phys. **63**, 239 (1991); J. A. Sauls, Adv. Phys. **43**, 1313 (1994).
 - [25] L. D. Landau, in *Collected Papers of L.D. Landau*, edited by D. ter Haar (Gordon and Breach, New York, 1967) p. 193.
 - [26] J. C. Ryan and A. K. Rajagopal: Phys. Rev. B **47**, 8843 (1993).
 - [27] A. Garg and D.-C. Chen, Phys. Rev. B **49**, 479 (1994).
 - [28] U. Yaron *et al.*, Phys. Rev. Lett. **78**, 3185 (1997).